Regioselectivity in lithiation of 1-methylpyrazole: experimental, density functional theory and multinuclear NMR study†

Thomas Balle,*[a] Mikael Begtrup,[a] Jerzy W. Jaroszewski,[a] Tommy Liljefors[a] and Per-Ola Norrby[b]

Received 12th December 2005, Accepted 20th January 2006
First published as an Advance Article on the web 3rd February 2006
DOI: 10.1039/b517607g

Reaction of 1-methylpyrazole with *n*-BuLi in THF followed by reaction with monodeuteromethanol (CH_3OD) under kinetically controlled conditions leads to functionalisation at the methyl group, whereas reaction under thermodynamically controlled conditions leads to functionalisation at the pyrazole 5-position. The observed regioselectivity can be correctly predicted, at least qualitatively, using density functional B3LYP/6-31+G(d,p) calculations only when solvation effects (IEFPCM) are taken into account. The $^{1}H,^{6}Li$ HOESY and NOESY NMR spectra of the thermodynamic product 5-lithio-1-methylpyrazole (**5-Li**) in [D_8]THF are consistent with an oligomeric structure.

Introduction

5-Membered nitrogen-containing heteroaromatics (azoles) can often be functionalized efficiently by lithiation followed by addition of an electrophile.[1] However, lithiation of different ring positions and exocyclic α-positions compete and the regioselectivity often depends on the reaction conditions. Prediction of the site of lithiation is instrumental in planning the synthesis of specific target molecules. Traditionally, this has been based on classical analysis of resonance structures.[2] However, these analyses fail when deprotonation of ring positions and α-positions compete. When the regioselectivity depends on the reaction conditions, kinetic and thermodynamic factors as well as solvent association may influence product distribution.[3] One such example is the lithiation of *N*-alkylpyrazoles.

Lithiation at the alkyl group in *N*-alkylpyrazoles occurs in competition with lithiation at the ring 5-position.[1,4–5] Depending on time, temperature, solvent and electrophile, the lithiation of 1-methylpyrazole (**1**) followed by reaction with an electrophile was reported to give 5-substituted products,[6–8] mixtures of α- and 5-substituted products[4,5,9] and mixtures of 3- and 5-substituted products.[10] Based on a study of the reactivity of 3- and 5-substituted 1-methylpyrazoles Katritzky *et al.* showed that lithiation at the α-carbon is kinetically controlled whereas lithiation at the pyrazole 5-position occurs under thermodynamic control.[5] Product distribution changes caused by different reactivity of various anionic species towards electrophiles and the fact that most product distributions were determined after work-up, *i.e.* extraction, chromatography or crystallisation, implies that the product distributions reported do not necessarily reflect the exact distribution of the intermediate anions at the time when they were quenched.

Theoretical calculations as a means of predicting regioselectivity in lithiation reactions have received considerable attention.[3,11–13] It has been shown that semi-empirical (PM3 and MNDO) as well as *ab initio* Hartree–Fock calculations are insufficient for prediction of the regioselectivity of lithiation of ring positions and exocyclic α-positions.[12] There seems to be a consensus in the literature that methods taking electron correlation into account are needed for this purpose.[14] Interestingly, hybrid methods based on density functional theory such as the B3LYP[15–17] method have been reported to give results in quantitative agreement with the more computationally demanding second-order Møller–Plesset (MP2) calculations.[14]

The choice of solvent may have a considerable influence on the regioselectivity in lithiation reactions.[18] At the theoretical level, solvation effects in lithiation reactions have either been studied by the introduction of explicit solvation[12,19,20] or by using a polarizable dielectric continuum[21] (PCM) model.[14] The recently reported IEFPCM model[22–25] based on the integral equation formalism[23,24,26] (IEF) is an attractive method for studying solvation effects in chemical reactions. The IEFPCM method includes electrostatic as well as cavitation, dispersion and repulsion terms in the calculation of the total free energy in solution. Though specific donor/acceptor orbital interactions between solvent and solute are not considered in the model, it does take into account electrostatic effects, which are considered to be the most important effects for solvation of lithium.[27] In addition, the model implements analytical derivatives making the method especially attractive for difficult geometry optimisation tasks such as transition state optimisations in solution.

We here present a study of the lithiation of 1-methylpyrazole (**1**) that compares lithiation monitored by ^{1}H, ^{6}Li and ^{13}C-NMR spectroscopy and deuterium labelling with density functional B3LYP calculations, considering various reaction pathways shown in Scheme 1. Solvation effects were taken into account by means of the IEFPCM solvation model for all compounds and compared to the effects of an explicit first solvation shell for two selected compounds. The results emphasise the importance of including solvent effects in calculations when aiming at the prediction of the regioselectivity of lithiation reactions.

[a]*Department of Medicinal Chemistry, The Danish University of Pharmaceutical Sciences, Universitetsparken 2, DK-2100, Copenhagen, (Denmark). E-mail: tb@dfuni.dk*
[b]*Department of Chemistry, Technical University of Denmark, DK-2800, Kgs. Lyngby, (Denmark)*

† Electronic supplementary information (ESI) available: atomic coordinates, absolute energies, zero-point energies and basis set superimposition error energies for geometries optimised in solution. See DOI: 10.1039/b517607g

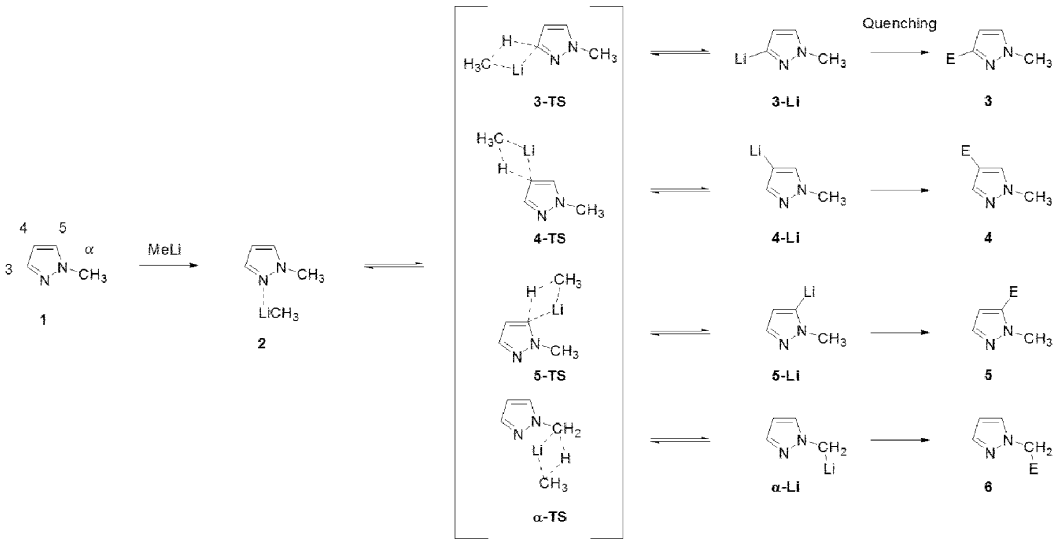

Scheme 1 Model for lithiation of 1-methylpyrazole.

Results

Hydrogen–deuterium exchange experiments

The results of lithiation of 1-methylpyrazole (**1**) in tetrahydrofuran (THF) at −78 °C using *n*-butyllithium (*n*-BuLi) followed by reaction with monodeuteromethanol (CH_3OD) are shown in Table 1. The differences in boiling points and solubilities of the products **1a** and **1b** and the starting material (**1**) are negligible. Therefore, the ratio between the constituents of the reaction mixture is not influenced by the work-up. The product distribution (site and extent of deuteration) was established by integration of the fully relaxed ^{1}H-NMR spectra. The measured integrals were normalised using the pyrazole H4 signal since H4 is not subject to exchange under the conditions used.[1]

The lithiation of 5-deutero-1-methylpyrazole (**1b**) containing 97% deuterium at the 5-position and 6% at the methyl group followed by reaction with methanol (CH_3OH) revealed 61% deuterium incorporation at the methyl group and 23% at the 5-position as determined by integration of the fully relaxed ^{1}H-NMR signals. Close examination revealed that the ^{1}H-NMR signals arising from the methyl group consisted of a singlet, a triplet and a quintet in the ratio 9 : 6 : 1.

Table 1 Lithiation of 1-methylpyrazole followed by reaction with CH_3OD

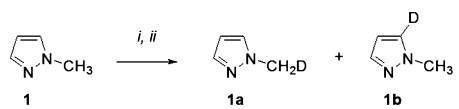

i) *n*-BuLi, THF, -78°C; *ii*) CH_3OD, -78°C to 20°C.

Reaction time		Product distribution yield (%) [a]	
(Min.)	Conversion of **1** (%)[a]	**1a**	**1b**
0.25	63	59	41
2	68	49	51
10	74	19	81
60	92	7	93

[a] Determined by ^{1}H-NMR.

Multinuclear NMR studies

1-Methylpyrazole (**1**) was lithiated at −78 °C using *n*-[^{6}Li]butyllithium in THF or [D_8]THF. ^{1}H-NMR spectra obtained at −20 °C showed the presence of **5-Li**, with resonances of H3, H4 and CH_3 at δ 7.11 (1 H), 5.85 (1 H) and 3.66 (3 H), respectively, with ^3J(H3,H4) = 1.6 Hz. The signals, as well as the corresponding ^{6}Li-NMR resonance, could be observed for at least 24 h without loss of intensity. Immediately after preparation, the solution exhibited additional, quickly vanishing resonances (broad singlets) at δ 7.03, 7.15 and 2.82 in the ratio of 1 : 1 : 2, attributable to H3, H5 and CH_2 of the kinetic reaction product **α-Li**; the H4 signal of the latter coincided with that of **5-Li**. The ^{13}C-NMR spectrum of the solution of **5-Li** (−20 °C) exhibited signals of C3, C4, C5 and CH_3 at δ 137.0, 115.2, 197.6 and 42.3, respectively; the low-field value of the chemical shift of C5 is in agreement with literature data.[28]

The ^{1}H,^{6}Li HOESY spectrum[29–31] of a solution of **5-Li** in [D_8]THF showed strong cross-peaks between the lithium resonance and the CH_3 group, and somewhat weaker cross-peaks to the H3 and H4 (Fig. 1). The integral volume ratio between the respective cross-peaks was 100 : 48 : 33. When the spectrum was recorded in non-deuterated THF, by far the strongest correlations observed were those to the solvent molecules, with cross-peaks to ring hydrogens relatively similar to those observed in [D_8]THF.

Longitudinal (T_1) relaxation times measured for **5-Li** using the inversion recovery method (−10 °C) were 3.0, 3.3 and 1.0 s for H3, H4 and CH_3, respectively. Relaxation times of the parent compound (**1**) determined at identical conditions were about 7 s for the ring protons and 4.3 s for the methyl group. A series of NOESY spectra recorded at −10 °C with mixing times in the range 25–700 ms showed that the **5-Li** molecule is in the negative NOE regime,[32] *i.e.*, exhibiting NOESY cross-peaks with the same phase as the diagonal. Interestingly, equally intense cross-peaks were observed for all correlations (Fig. 2), and NOE build-up curves for all proton pairs were closely similar (Fig. 3).

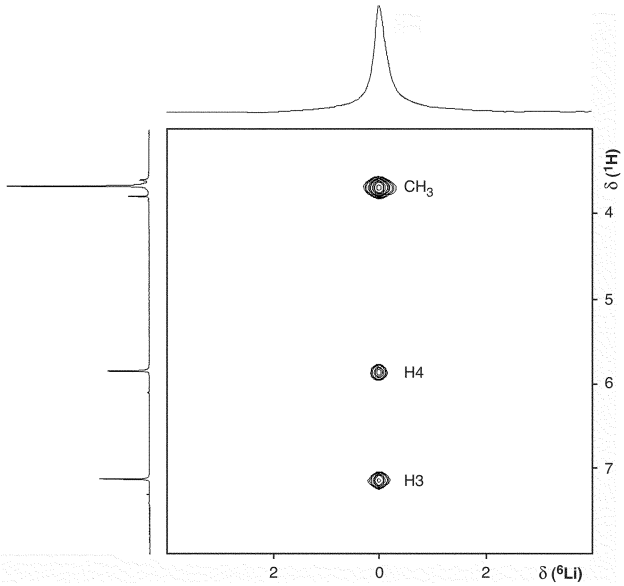

Fig. 1 $^{1}H,^{6}Li$ HOESY spectrum of **5-Li** in [D_8]THF at −10 °C (59 MHz, mixing time 2 s).

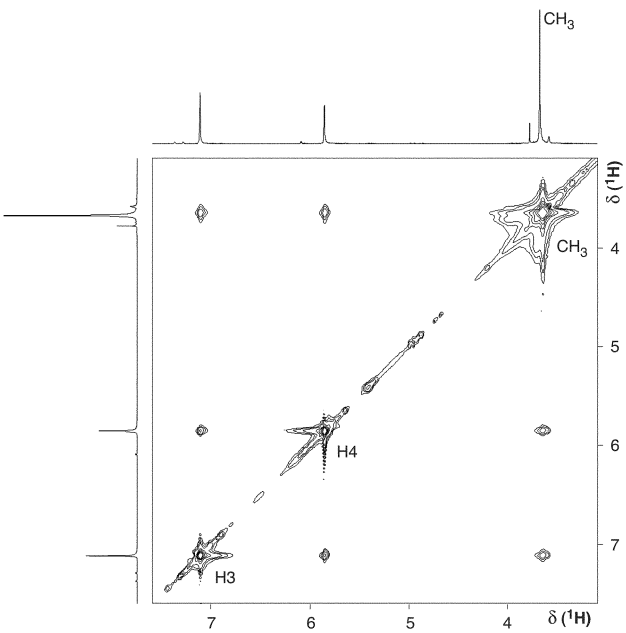

Fig. 2 NOESY spectrum of **5-Li** in [D_8]THF at −10 °C (400 MHz, mixing time 100 ms).

Calculations

Prediction of the regioselectivity for the lithiation of 1-methylpyrazole (**1**) with *n*-BuLi followed by reaction with an electrophile requires prediction of both the kinetically and the thermodynamically favored product.

We have therefore investigated the stationary points along the reaction coordinate by means of quantum mechanical calculations. Theoretically, 1-methylpyrazole (**1**) may react with *n*-BuLi at the three ring positions or at the methyl group. Prediction of the regioselectivity of the lithiation of 1-methylpyrazole (**1**) thus requires comparison of the relative energies of the four different transition states **3-TS**, **4-TS**, **5-TS** and **α-TS** as well as of the four

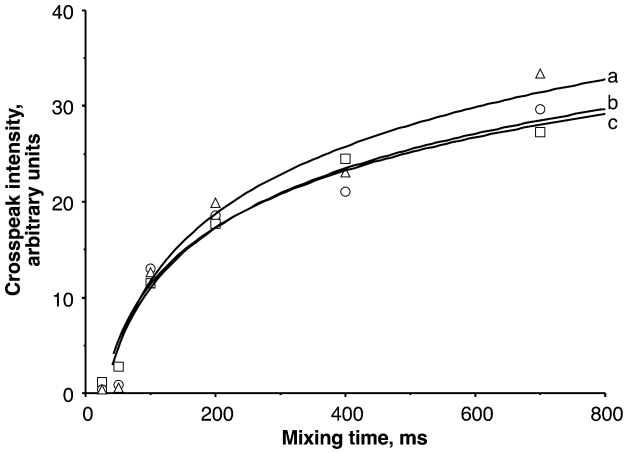

Fig. 3 NOE build-up curves for **5-Li** (−10 °C, [D_8]THF, 400 MHz); triangles (curve a), circles (curve b) and squares (curve c), represent NOESY integral peak volumes for correlations between CH_3 and H3, CH_3 and H4, and H3 and H4, respectively.

different lithiated intermediates **3-Li**, **4-Li**, **5-Li** and **α-Li** shown in Scheme 1.

In the calculations of geometries and energies of transition states, methyllithium (MeLi) was used as a model for *n*-BuLi used experimentally (see below) in order to reduce the size and flexibility of the system. In addition, all species including the transition states were assumed to be monomeric, neglecting that alkyl- and aryl lithiums may form aggregates in THF solution.[31] The final calculations were performed with the hybrid density functional method B3LYP using the 6-31+G(d,p) split valence basis set that includes diffuse functions. All geometries were first optimised in the gas phase. Solvation effects were taken into account using the IEFPCM method, specifying THF as solvent. Atomic radii optimised for the PBE0 level of theory[33] were obtained from the united atom topological model.[34] Initially, single point total energies in solution were calculated for the gas phase structures, followed by calculation of total free energies in solution by geometry optimisation within the IEFPCM framework. Analytical frequency calculations were performed for all structures to confirm that the structures were either energy minima or transition states. The effect of explicit THF coordination was investigated by comparing the energy of **5-Li** coordinating three molecules of THF (**5-Li**·3THF) to the energy of **α-Li** coordinating two molecules of THF (**α-Li**·2THF + THF). Geometries and energies for these species were optimised within the IEFPCM framework and are counterpoise corrected to allow for the direct comparison of the energies of these two systems. For structural details of the compounds and intermediates discussed in the present paper the reader is referred to the electronic supplementary information (ESI)† where *xyz* coordinates and absolute energies are reported.

Initial complex

Coordination of MeLi to N2 of 1-methylpyrazole (**1**) initially leads to a C_s-symmetrical complex (**2**) stabilised by 21.1 kcal mol^{-1} relative to the energy of the individual reactants (**1** + MeLi) in the gas phase and by 10.9 kcal mol^{-1} in the solvent (Table 2). The geometries in the gas phase and in the solvent did not differ significantly.

Table 2 Calculated energies[a] (kcal mol^{-1}), relative to initial complex **2**

Energy:[a]	B3LYP	IEFPCM/B3LYP	IEFPCM/B3LYP
Geometry:	B3LYP	B3LYP	IEFPCM/B3LYP
Reactants			
1 + MeLi	21.1	10.9	10.8
Initial complex			
2	0	0	0
Transition structures (relative to α-**TS**)			
3-TS	23.9 (6.8)	22.5 (3.9)	22.1 (3.7)
4-TS	33.2 (16.1)	28.5 (9.9)	28.1 (9.8)
5-TS	31.2 (14.2)	26.4 (7.8)	25.9 (7.5)
α-**TS**	17.1 (0.0)	18.6 (0.0)	18.4 (0.0)
Products (relative to α-**Li**)			
3-Li + CH_4	5.3 (9.1)	−1.2 (4.9)	−0.5 (5.9)
4-Li + CH_4	11.6 (15.3)	−1.0 (5.1)	−1.3 (5.1)
5-Li + CH_4	7.8 (11.6)	−6.4 (−0.3)	−6.7 (−0.3)
α-**Li** + CH_4	−3.8 (0.0)	−6.1 (0.0)	−6.4 (0.0)
Explicit solvation for selected products (relative to α-**Li**·2THF + THF)[a,b]			
5-Li·3THF			(−3.6)
α-**Li**·2THF + THF			(0.0)

[a] Energy corrected for ZPE; Basis set: 6-31+G(d,p). [b] Counterpoise corrected.

Transition states

All transition state structures display C_1-symmetry except **3-TS**, which shows C_s-symmetry. The four transition states all display an almost neutral hydrogen situated approximately midway between the two reactants, giving the deprotonation the character of a hydrogen transfer process.[35] In all cases lithium is situated outside the reaction centre. In the gas phase, the energies of the transition states decrease in the order **4-TS** > **5-TS** > **3-TS** > α-**TS** (Table 2). The same order of energies is observed in solvent, irrespective of whether the geometries were reoptimised or not. The relative energies compared to α-**TS** are reduced by up to 3 kcal mol^{-1} as a result of solvation. In the two most stable transition state structures, **3-TS** and α-**TS**, lithium is coordinated to N2 of the pyrazole ring.

Lithiated intermediates

All lithiated species, **3-Li**, **4-Li**, **5-Li** and α-**Li**, have C_s-symmetrical energy minima. The gas phase energies decrease in the order **4-Li** > **5-Li** > **3-Li** ≫ α-**Li** (Table 2). **3-Li** and α-**Li** exhibit strong coordination of lithium to N2 of the pyrazole. These species are less stabilised by solvation compared to **4-Li** and **5-Li**, which lack internal coordination to N2. Simple estimation of the solvated energies using the gas phase geometries give the ranking **4-Li** > **3-Li** > α-**Li** > **5-Li**. However, geometry optimisation in solvent changed the geometries and relative energies: The 3-lithiated species **3-Li** loses the coordination between lithium and N2, and thus gains much less than the other species from the optimisation. As a result, the predicted total energies in solvent decrease in the order **3-Li** > **4-Li** ≫ α-**Li** > **5-Li**. The effect of explicit THF solvation was investigated for the two most stable lithiated intermediates α-**Li** > **5-Li** by comparing the energies of α-**Li**·2THF + THF and **5-Li**·3THF (Table 2). For these species, the total energy in solvent decreases in the order α-**Li**·2THF + THF > **5-Li**·3THF.

Discussion

Hydrogen deuterium exchange experiments

The results in Table 1 show that deuteration of 1-methylpyrazole (**1**) initially takes place at the methyl group (**1a**), the deuterium incorporation at the pyrazole 5-position (**1b**) is considerably slower. This demonstrates that a prototopic shift from Me to C5 takes place. Accordantly, lithiation of 5-deutero-1-methylpyrazole (**1b**) and subsequent quenching with methanol (CH_3OH) gave rise to a transfer of deuterium from C5 to the methyl group to an extent of 61%. The presence of a singlet, a triplet and a quintet indicates the presence of a CH_3, a CH_2D and CHD_2 group in the ratio 3 : 3 : 1. Intermolecular transfer of lithium from the *N*-methyl group to the pyrazole 5-position *involving* **1** accounts for these observations. The present results confirm that lithiation of 1-methylpyrazole (**1**) occurs at the α-position under kinetic control and is followed by an intermolecular hydrogen transfer to the thermodynamically more favoured 5-lithiated derivative **5-Li**.

Transition states

The gas phase energies for the transition states decrease in the order **4-TS** > **5-TS** > **3-TS** > α-**TS** as shown in Fig. 4. The two transition states with the lowest energy, α-**TS** and **3-TS**, are apparently stabilised by strong coordination of lithium to N2. The effect of solvation of the transition states **3-TS**, **4-TS** and **5-TS** is larger than that of α-**TS**, as shown in Fig. 4. However, taking solvation into account does not change the predicted regioselectivity of the reaction.

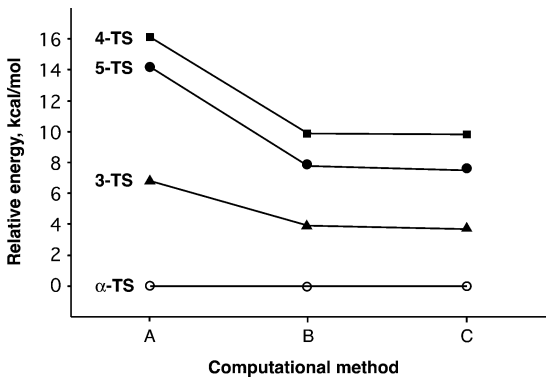

Fig. 4 Relative energy for transition states calculated using the B3LYP/6-31+G(d.p)method. (A): Gas phase energy; (B): Total energy in solution (gas phase structures); (C): Total energy in solution (solution phase structures).

Lithiated intermediates

The energies of the lithiated intermediates **3-Li**, **4-Li**, **5-Li** and α-**Li** are heavily influenced by solvation (Fig. 5). In the gas phase **3-Li** and especially α-**Li**, both exhibiting strong coordination of lithium to N2, are the most stable species. However, these species are affected significantly less by solvation compared to **4-Li** and in particular to **5-Li**. **5-Li** is predicted to be the most stable species in solution, but its relative energy is closely similar to that of α-**Li**. Interestingly, the coordination between lithium and N2 in the 3-lithiated intermediate **3-Li** is broken during geometry optimisation, suggesting that the solvation model is sufficiently

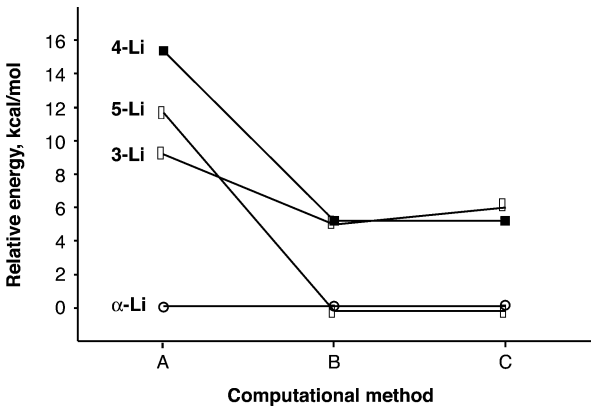

Fig. 5 Relative energy for products calculated using the B3LYP/6-31+G(d,p) method. (A): Gas phase energy; (B): Total energy in solution (gas phase structures); (C): Total energy in solution (solution phase structures).

strong to approximate the electrostatic effect of coordination. The resulting predicted order of reactivity of **3-Li** and **4-Li** is reversed compared to the solvated single point energies based on the gas phase optimised structures. The total energies in solution after geometry optimisation decrease in the order **3-Li** > **4-Li** ≫ **α-Li** > **5-Li**, the 5-lithiated species **5-Li** being 0.3 kcal mol^{-1} more stable compared to **α-Li**. When considering explicit solvation of **α-Li** and **5-Li**, the two most stable species in solvent, the 5-lithiated intermediate **5-Li**·3THF is favored over **α-Li**·2THF + THF by *ca.* 3 kcal mol^{-1}.

Reactivity

The calculated reaction profiles for the structures optimised in THF, shown in Fig. 6, indicate that lithiation at the exocyclic *α*-position occurs under kinetic control in agreement with experimental results. The energies of the transition states leading to direct lithiation of the pyrazole 4- and 5-positions (**4-TS** and **5-TS**) are 9.8 and 7.5 kcal mol^{-1} higher as compared to the energy of **α-TS**. Therefore, lithiation at these positions is unlikely to occur when the reaction is run under kinetic control. Due to the stabilizing effect of the interaction of N2 with Li, **3-TS** is only 3.7 kcal mol^{-1} above **α-TS** in energy. At −78 °C, this corresponds to a reactivity difference of around four orders of magnitude. No 3-deutero-1-methylpyrazole was observed in the lithiation and quenching

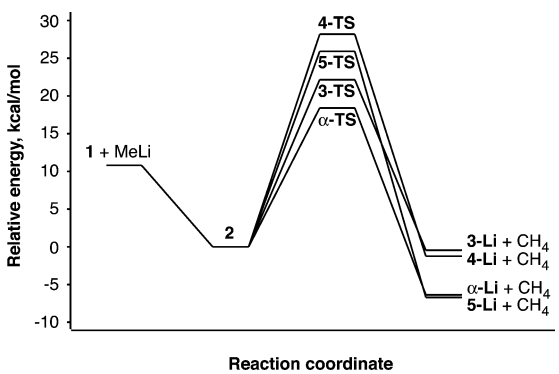

Fig. 6 Reaction coordinate in THF solution [IEFPCM/B3LYP/6-31 + G(d,p)], relative to **2** (solution phase structures).

experiments (Table 1), but the sensitivity of the analysis by ^{1}H-NMR used in the present work is insufficient to detect a degree of deuteration below 5%. Azami *et al.*[10] have isolated 3- and 5-hydroxymethyl-1-methylpyrazole in the ratio 4 : 96 after reaction of 1-methylpyrazole with excess of *n*-BuLi followed by reaction with DMF and subsequent reduction with $NaBH_4$. The presence of a large excess of *n*-BuLi does indeed favour kinetic control since it suppresses the presence of unreacted 1-methylpyrazole (**1**) which is catalysing the formation of the thermodynamically favoured species **5-Li**. The thermodynamic product is correctly predicted by the calculations to be the 5-lithiated compound **5-Li**, closely followed by **α-Li**. However, the predicted small energy difference between **α-Li** and **5-Li** of 0.3 kcal mol^{-1} is too low to account for the product distribution of 7 : 93 (Table 1) observed after 60 min. The inclusion of explicit solvation gives qualitatively similar results, but predicts the energy difference between the two species to be 3.6 kcal mol^{-1}, which is in better agreement with the observed product distribution described above.

The computational predictions could be fully confirmed by NMR-spectroscopic results. Thus, stable **5-Li** species were observed in THF solutions at sub-zero temperatures, and could be characterized by ^{1}H-, ^{6}Li- and ^{13}C-NMR. Freshly prepared mixtures of **1** and *n*-BuLi indeed contained a product with ^{1}H-NMR resonances compatible with the structure of **α-Li**, which rapidly vanished with concomitant formation of **5-Li**. No other species were observed by low-temperature ^{1}H-NMR, neither in the initial nor in the equilibrated reaction mixture, except for an excess of starting material (**1**) in some cases.

Solutions of **5-Li**, enriched with ^{6}Li, gave a HOESY spectrum demonstrating close proximity not only between Li and CH_3 and H4, but also between Li and H3 (Fig. 1). In fact, the correlation between Li and H3 was stronger than that to H4. Moreover, strong HOESY correlations between lithium and solvent molecules were observed (data not shown). NOESY spectra showed equally intense cross-peaks between all hydrogen pairs in the molecule even at mixing times very much shorter than their longitudinal relaxation times measured at the same conditions. These results, and the observation of negative NOE's for **5-Li** demonstrate the presence of a molecular aggregate with substantially decreased mobility. Although the NOESY spectra may to some extent be affected by spin diffusion, the observed homo- and heteronuclear NOE connectivities must in part be due to intermolecular relaxation, demonstrating the presence of a molecular aggregate consisting of several **5-Li** molecules as well as THF molecules. The structure of the cluster cannot be derived from the available data, which nevertheless suggest a coordination of lithium from one **5-Li** molecule to nitrogen of another molecule or molecules. The formation of Li-bridged fluxional clusters is well established for organolithium compounds.[31,36]

Conclusion

The present results have confirmed experimentally that in THF, 1-methylpyrazole (**1**) is lithiated at the exocyclic *α*-position, and that the initially formed *α*-lithiated species form the thermodynamic product **5-Li** in an intermolecular reaction. Although NOESY and HOESY data confirm the expected presence of a lithium-bridged and THF-solvated oligomer, the regioselectivity could be predicted correctly by B3LYP/6-31+G(d,p) calculations utilizing

full geometry optimisation within the IEFPCM framework, using monomeric species as models. A coordination from N2 to lithium is apparently favoring formation of the kinetic product **α-Li**.

Experimental

General methods

All reactions were performed under nitrogen using syringe-septum cap techniques. All glassware was flame-dried prior to use. THF was freshly distilled over sodium/benzophenone.

Materials

All materials were obtained from commercial suppliers, except *n*-[^{6}Li]BuLi, which was prepared as reported previously using ^{6}Li enriched to 95%.[37] *n*-BuLi was titrated prior to use.[38]

Lithiation of 1-methylpyrazole (1) and trapping of lithiated species. 1-Methylpyrazole (**1**) (60.0 mg, 0.74 mmol) in THF (10 mL) was cooled to −78 °C. *n*-BuLi (0.56 mL, 1.6 M in hexanes, 1.2 equivalents) was added at constant rate during 2 min. The solutions were stirred at −78 °C for 0.25, 2, 10 and 60 min, respectively, and quenched with CH_3OD (0.1 mL). The cooling bath was removed and the solution stirred until it reached room temperature. Aqueous HCl (0.2 mL, 12 M) was added, and the solvents were removed at reduced pressure (40 °C, 20 mbar). D_2O (1 mL) and $CDCl_3$ (1 mL) were added, and the solution neutralised by addition of $NaHCO_3$. The phases were separated by centrifugation and the $CDCl_3$ solution was transferred to an NMR tube for analysis.

5-Deutero-1-methylpyrazole (1b). A solution of 1-methylpyrazole (**1**) (1.04 g, 12.7 mmol) and THF (70 mL) was cooled to −78 °C. *n*-BuLi (9.9 mL, 1.6 M in hexanes, 1.25 equivalents) was added at a constant rate during 2 min. The solution was stirred at −78 °C for 5 min and at 23 °C (water bath) for 1 h before addition of CH_3OD (2 mL). The solution was stirred for 1 h before addition of aqueous HCl (2 mL, 12 M) and subsequent evaporation of the solvents as above. The remaining oil was dissolved in H_2O (10 mL) and neutralised with $NaHCO_3$. The aqueous phase was extracted with diethyl ether (4 × 4 mL). The solution was distilled (Vigreux column, ambient pressure) and the final product collected between 125–128 °C (reported for 1-methylpyrazole (**1**) after redistillation over Na: 126–127 °C).[39] Yield 0.56 g (53%). ^{1}H-NMR ($CDCl_3$): δ = 7.48 (d, J(H3,H4) = 1.6 Hz, 1 H), 7.34 (s, broad, 0.03 H), 6.23 (d, J(H4,H3) = 1.6 Hz, 1 H), 3.90 (s, 2.94 H).

Lithiation of 5-deutero-1-methylpyrazole (1b). 5-Deutero-1-methylpyrazole (**1b**) was lithiated as described above for **1**, except the solution was stirred for 5 min at −78 °C and 60 min at 23 °C before addition of CH_3OH.

NMR spectroscopy

Samples for NMR spectroscopy were obtained by mixing 1-methylpyrazole (**1**) (17.2 mg, 0.23 mmol) in THF or [D_8]THF (0.55 ml, containing tetramethylsilane) with *n*-[^{6}Li]BuLi (0.13 mL, 1.94 M in pentane, 1.1 equivalent) in a 5 mm NMR tube at −78 °C. The solution was investigated immediately or shaken vigorously at room temperature for 10 min to obtain equilibrium mixture; if necessary, the tube was stored in liquid nitrogen until the NMR experiment was performed. ^{1}H-, ^{6}Li- and ^{13}C-NMR spectra were obtained on a Bruker AMX400 instrument at 400.13, 58.88 and 100.62 MHz, respectively, using 5 mm broad-band inverse-configuration probe-head cooled with a stream of liquid nitrogen vapour. Temperature was controlled with a calibrated variable temperature unit and is believed to be accurate within 2 K. ^{1}H- and ^{13}C-NMR spectra were referenced to internal tetramethylsilane, whereas ^{6}Li-NMR shifts are unreferenced. HOESY spectra were acquired in phase-sensitive mode collecting 64 transients with 2 k data points for each of 128 increments, using 2 s mixing time and 12 s relaxation delay. The spectra were transformed with zero filling by a factor of two in the indirect dimension. Phase sensitive NOESY spectra were acquired with 25–700 ms mixing times, collecting 16 transients with 1 k data points in 512 increments, zero filled to 1 k. Waltz16-decoupled ^{13}C-NMR spectra were acquired using standard procedures. Quantitative (fully relaxed) spectra were recorded using 20° pulses with inter-pulse delay of 12 s. Longitudinal (T_1) relaxation times were determined using inversion recovery pulse sequence with approx. 20 values of relaxation delay (t); T_1 was determined by fitting line intensities into three-parameter equation [Intensity = ConstantA + ConstantB × exp($-t/T_1$)].

Computational methods

Ab initio calculations were carried out using Gaussian 03.[34] All calculations were performed using the 6-31+G(d,p) basis set requiring tight convergence of the self-consistent field. For B3LYP calculations an ultra fine grid was specified. For transition state optimisations force constants were recalculated analytically at each optimisation step. Vibrational frequencies were calculated analytically to verify the structures as minima or transition states. Zero-point energies (ZPE's) were extracted from the frequency calculations and were used unscaled. All reported energies are corrected for ZPE's. For all transition structures a forced 0.01 Å contraction and extension along the reaction coordinate and a following geometry optimisation lead to reactants (initial complex) and products, respectively. Total free energies in solution were calculated using the IEFPCM procedure specifying THF as solvent. Radii optimised for the PBE0 level of theory[33] were obtained from the united atom topological model.[34] Total free energies in solution were calculated for the gas phase structures and for the structures optimised within the IEFPCM model. The first solvation shell of **5-Li**·3THF and **α-Li**·2THF was adapted from the X-ray structures ZELDUP[40] and TUMPOG01,[41] respectively, and subsequently geometry optimised using the IEFPCM procedure as described above.

Acknowledgements

This work was supported by the Lundbeck Foundation, the Danish Natural Science Research Council (Grant No. 9503673) and the Danish Technical Research Council. We thank Dr. Ebbe Kelstrup and Dr. Helge Johansen for valuable criticism and suggestions during the initial part of the project.

References

1 M. R. Grimmett and B. Iddon, *Heterocycles*, 1994, **37**, 2087–2147.
2 M. Begtrup, *Heterocycles*, 1992, **33**, 1129–1153.
3 M. C. Whisler, S. MacNeil, V. Snieckus and P. Beak, *Angew. Chem., Int. Ed.*, 2004, **43**, 2206–2225.
4 D. E. Butler and S. M. Alexander, *J. Org. Chem.*, 1972, **37**, 215–220.
5 A. R. Katritzky, C. Jayaram and S. N. Vassilatos, *Tetrahedron*, 1983, **39**, 2023–2029.
6 R. Hüttel and M. E. Schön, *Justus Liebigs Ann. Chem.*, 1959, **625**, 55–65.
7 K. Yagi, T. Ogura, A. Numata, S. Ishii and K. Arai, *Heterocycles*, 1997, **45**, 1463–1466.
8 T. Balle, K. Andersen and P. Vedsø, *Synthesis*, 2002, 1509–1512.
9 F. Effenberger and A. Krebs, *J. Org. Chem.*, 1984, **49**, 4687–4695.
10 H. Azami, D. Barrett, A. Tanaka, H. Sasaki, K. Matsuda, M. Sakurai, T. Terasawa, F. Shirai, T. Chiba, Y. Matsumoto and S. Tawara, *Bioorg. Med. Chem.*, 2001, **9**, 961–982.
11 T. Kremer, M. Junge and P. v. R. Schleyer, *Organometallics*, 1996, **15**, 3345–3359.
12 A. Opitz, R. Koch, A. R. Katritzky, W.-Q. Fan and E. Anders, *J. Org. Chem.*, 1995, **60**, 3743–3749.
13 B. V. Cheney, *J. Org. Chem.*, 1994, **59**, 773–779.
14 E. L. Coitiño, E. Ciuffarin, F. M. Floris and J. Tomasi, *J. Phys. Chem. A*, 1998, **102**, 8369–8376.
15 A. D. Becke, *J. Chem. Phys.*, 1993, **98**, 5648–5652.
16 C. Lee, W. Yang and R. G. Parr, *Phys. Rev. B: Condens. Matter*, 1988, **37**, 785–789.
17 P. J. Stephens, F. J. Devlin, C. F. Chablowski and M. J. Frisch, *J. Phys. Chem.*, 1994, **98**, 11623–11627.
18 D. W. Slocum, S. Dumbris, S. Brown, G. Jackson, R. LaMastus, E. Mullins, J. Ray, P. Shelton, A. Walstrom, J. M. Wilcox and R. W. Holman, *Tetrahedron*, 2003, **59**, 8275–8284.
19 (*a*) J. Morey, A. Costa, P. M. Deyá, G. Suñer and J. M. Saá, *J. Org. Chem.*, 1990, **55**, 3902–3909; (*b*) J. M. Saá, P. M. Deyá, G. A. Suñer and A. Frontera, *J. Am. Chem. Soc.*, 1992, **114**, 9093–9100; (*c*) J. M. Saá, G. Martorell and A. Frontera, *J. Org. Chem.*, 1996, **61**, 5194–5195.
20 J. M. Saá, J. Morey, A. Frontera and P. M. Deyá, *J. Am. Chem. Soc.*, 1995, **117**, 1105–1116.
21 S. Miertus, E. Scrocco and J. Tomasi, *Chem. Phys.*, 1981, **55**, 117–129.
22 M. Cossi, V. Barone, B. Mennucci and J. Tomasi, *Chem. Phys. Lett.*, 1998, **286**, 253–260.
23 E. Cancès, B. Mennucci and J. Tomasi, *J. Chem. Phys.*, 1997, **107**, 3032–3041.
24 B. Mennucci, E. Cancès and J. Tomasi, *J. Phys. Chem. B*, 1997, **101**, 10506–10517.
25 J. Tomasi, B. Mennucci and E. Cancès, *THEOCHEM*, 1999, **464**, 211–226.
26 E. Cancès and B. Mennucci, *J. Math. Chem.*, 1998, **23**, 309–326.
27 R. P. Quirk, D. E. Kester and R. D. Delaney, *J. Organomet. Chem.*, 1973, **59**, 45–52.
28 R. R. Fraser, T. S. Mansour and S. Savard, *Can. J. Chem.*, 1985, **63**, 3505–3509.
29 P. L. Rinaldi, *J. Am. Chem. Soc.*, 1983, **105**, 5167–5168.
30 C. Yu and G. C. Levy, *J. Am. Chem. Soc.*, 1984, **106**, 6533–6537.
31 W. Bauer, in *Lithium Chemistry, a Theoretical and Experimental Overview*, ed. A. M. Sapse and P. v. R. Schleyer, John Wiley & Sons, New York, 1995, pp. 125–172.
32 D. Neuhaus and M. P. Williamson, *The Nuclear Overhauser Effect in Structural and Conformational Analysis*, VCH, Weinheim, 1989.
33 C. Adamo and V. Barone, *J. Chem. Phys.*, 1999, **110**, 6158–6170.
34 M. J. Frisch, G. W. Trucks, H. B. Schlegel, G. E. Scuseria, M. A. Robb, J. R. Cheeseman, J. J. A. Montgomery, T. Vreven, K. N. Kudin, J. C. Burant, J. M. Millam, S. S. Iyengar, J. Tomasi, V. Barone, B. Mennucci, M. Cossi, G. Scalmani, N. Rega, G. A. Petersson, H. Nakatsuji, M. Hada, M. Ehara, K. Toyota, R. Fukuda, J. Hasegawa, M. Ishida, T. Nakajima, Y. Honda, O. Kitao, H. Nakai, M. Klene, X. Li, J. E. Knox, H. P. Hratchian, J. B. Cross, C. Adamo, J. Jaramillo, R. Gomperts, R. E. Stratmann, O. Yazyev, A. J. Austin, R. Cammi, C. Pomelli, J. W. Ochterski, P. Y. Ayala, K. Morokuma, G. A. Voth, P. Salvador, J. J. Dannenberg, V. G. Zakrzewski, S. Dapprich, A. D. Daniels, M. C. Strain, O. Farkas, D. K. Malick, A. D. Rabuck, K. Raghavachari, J. B. Foresman, J. V. Ortiz, Q. Cui, A. G. Baboul, S. Clifford, J. Cioslowski, B. B. Stefanov, G. Liu, A. Liashenko, P. Piskorz, I. Komaromi, R. L. Martin, D. J. Fox, T. Keith, M. A. Al-Laham, C. Y. Peng, A. Nanayakkara, M. Challacombe, P. M. W. Gill, B. Johnson, W. Chen, M. W. Wong, C. Gonzalez and J. A. Pople, *Gaussian 03 Rev. B.02*, Gaussian Inc., Pittsburgh PA, 2003.
35 R. P. Bell, *The Tunnel Effect in Chemistry*, Chapman and Hall, London, 1980.
36 A. Streitweiser, S. M. Bachrach, A. Dorigo and P. v. R. Schleyer, in *Lithium Chemistry, a Theoretical and Experimental Overview*, ed. A. M. Sapse and P. v. R. Schleyer, John Wiley & Sons, New York, 1995, pp. 1–43.
37 G. Hilmersson and Ö. Davidsson, *J. Organomet. Chem.*, 1995, **489**, 175–179.
38 J. Suffert, *J. Org. Chem.*, 1989, **54**, 509–510.
39 M. Begtrup and P. Larsen, *Acta Chem. Scand.*, 1990, **44**, 1050–1057.
40 T. Kottke, K. Sung and R. J. Lagow, *Angew. Chem., Int. Ed. Engl.*, 1995, **34**, 1517–1519.
41 C. Eaborn, P. B. Hitchcock, J. D. Schmith and S. E. Sözerli, *Organometallics*, 1998, **17**, 4322–4325.